EFFECT OF BIAXIAL LOADING AND GEOMETRY ON PREDICTION OF LOW-CYCLE FATIGUE LIFE

A. W. A. KONTER, G. T. M. JANSSEN

T.N.O., Institute for Mechanical Constructions, P.O. Box 29, 2600 AA Delft, The Netherlands

W. HUSSLAGE

T.N.O., Metal Research Institute, P.O. Box 541, 7300 AM Apeldoorn, The Netherlands

Summary

Data to predict failure by low-cycle fatigue are mainly based on uniaxial constant amplitude tests on solid specimens, although in practically all cases the state of stress of a reactor component is multiaxial. The effect of multiaxiality has been investigated on thin-walled tubular specimens. For the uniaxial loading condition a comparison has been made with tests on solid specimens.

The investigated materials were 18Cr-11Ni steel (type AISI 304) at 20^{0}C and 550^{0}C and Nb-stabilized 2¼Cr1Mo steel at 550^{0}C. The thin-walled tubular specimens have been loaded by combinations of cyclic axial load and cyclic torsion, with which a range of principal stress ratios between $-1 \leq \sigma_2/\sigma_1 \leq 0$ or principal strain ratios between $-1 \leq \Delta\varepsilon_2/\Delta\varepsilon_1 \leq -0.5$ could be achieved.

It appeared both from the results and from literature that none of the classical criterions (like VON MISES, TRESCA) are adequate to describe fatigue life on basis of an equivalent strain. On basis of work of BROWN and MILLER, who indicated that the prevailing parameters in low-cycle fatigue are the maximum shear strain $\Delta\varepsilon_s$ and the strain $\Delta\varepsilon_n$ normal to the plane of maximum shear, a modification of the VON MISES criterion is proposed, which is formulated in terms of $\Delta\varepsilon_s$ and $\Delta\varepsilon_n$. In this criterion the ratio of axial strain of a push/pull test and shear strain of a torsion test giving equal fatigue life has been introduced as a parameter. Application of the criterion gave a good agreement for the results on both materials. An extrapolation can be given for specimens loaded in the range $-0.5 \leq \Delta\varepsilon_2/\Delta\varepsilon_1 \leq 1$. With this extrapolation reasonable agreement was obtained on available data in literature.

If the same axial strain range is applied, a remarkable reduction in fatigue life is observed for the tubular specimens in comparison with the solid specimens. With an elastic-plastic analysis a complete load cycle has been analysed for both types of specimen.
The calculated strain ranges have been verified experimentally. The strain concentrations are significant. The tubular specimen showed the highest strain concentrations on the inner surface; they were nearly equal to the strain concentrations on the surface of the solid specimen. Therefore, the difference in life could not be explained by strain concentrations.

With fractography it appeared that differences in fatigue life are influenced by crack initiation and crack growth. Crack initiation is affected by the surface finish. Crack growth, measured by counting of striation spacings, is influenced by the number of crack nucleation sites and the specimen geometry.

1. Introduction

In fast breeder reactors plastic and/or creep deformations may occur during operations, during start-up and shut-down procedures and other transients and during emergency situations. In the ASME Code N-47 /1/ limits are set to the deformations and number of allowable fatigue cycles, whereas the damage as a result of the interaction of creep and plasticity is restricted by an interaction rule. The criterions for fatigue have mainly been based on uniaxial constant amplitude low-cycle fatigue tests on solid specimens. It is not clear, whether the treatment of fatigue under multiaxial states of stress with the recommended VON MISES criterion is sufficiently accurate or at least conservative.

As part of a research program directed on inelastic analysis and life prediction at elevated temperatures, which includes a.o. creep, fatigue and their interaction under multiaxial loading conditions, the effect of biaxial states of stress on low-cycle fatigue is considered The experiments have been performed on two structural steels for the prototype LMFBR SNR-300.

2. Materials, experimental technique and specimens

The investigation has been performed on two structural steels. One is an austenitic 18Cr-11Ni steel (WN 1.4948, type AISI 304) tested at $20^{\circ}C$ and $550 \pm 0.5^{\circ}C$, the other one is a ferritic Nb-stabilized $2\frac{1}{4}$Cr1Mo steel (WN 1.6770) tested at $550 \pm 0.5^{\circ}C$. The composition of the steels and some characteristic mechanical properties are given in the Tables 1 and 2 respectively.

The specimens, shown in Figure 1, had a small curvature over the gauge length to promote failure in the middle of the specimens. The tests were carried out on a servo-hydraulic closed-loop testing machine, provided with an axial and torsional actuator. All tests were controlled on total strain with a triangular wave shape and a strain rate of $0.15\%.s^{-1}$. Tests were carried out in push/pull, in torsion and a combination of both (in-phase).

During each experiment a number of hysteresis-loops were recorded for axial and shear deformations. The number of cycles to failure N_f has been defined as the number of cycles where one of the maximum stresses, which can either be the tensile, compressive or shear stress, has decreased 25 % with respect to its value at about $\frac{1}{2}N_f$ as a result of macrocracking. An example of the maximum stresses in a combined test is shown in Figure 2.

On broken specimens, crack growth measurements have been performed by means of countings of striation spacings with the aid of scanning electron micrographs.

3. Effect of biaxial loading on low-cycle fatigue

Although the experiments have been carried out in a total strain controlled mode, a formulation in terms of plastic strains has been taken, since the damage is caused by plastic strains. Moreover the plastic volumetric change can be neglected. From the recorded hysteresisloops the average plastic strainrange during the experiment has been determined. For each ratio of principal plastic strains parallel to the surface $\xi = \Delta\varepsilon_{p2}/\Delta\varepsilon_{p1}$ the maximum principal plastic strain $\Delta\varepsilon_{p1}$ versus the number of cycles to failure has been plotted (Figure 3). For each ratio ξ it is assumed that the results can be described by the COFFIN-MANSON relation

$$\Delta\varepsilon_{p1} = C.N_f^{\alpha} \qquad (1)$$

The values of the constants C en α are listed in Table 3.

BROWN and MILLER /2/ cited various criterions to relate a multiaxial stress state to a uniaxial one. They argued that the prevailing parameters in the description of multiaxial low-cycle fatigue life are the maximum plastic shearstrain range $\Delta\varepsilon_{p,s}=(\Delta\varepsilon_{p,max}-\Delta\varepsilon_{p,min})/2$ and the strain range normal to the plane of maximum shear $\Delta\varepsilon_{p,n}=(\Delta\varepsilon_{p,max}+\Delta\varepsilon_{p,min})/2$. For biaxial stress states $\Delta\varepsilon_{p,max}$ is always parallel to the surface, while $\Delta\varepsilon_{p,min}$ can be either parallel (Case A) or perpendicular to the surface (Case B). Case A corresponds to ratios of principal strains $-1 \leq \xi \leq -0.5$ and Case B to $-0.5 \leq \xi \leq 1$. For Case A the cracks propagate predominantly along the surface of the specimen. For Case B the cracks extend predominantly in depth. For uniaxial loading ($\xi = -0.5$) often a circular crackfront is found.

The most frequently used definitions of equivalent strains can be written in terms of $\Delta\varepsilon_{p,n}$ and $\Delta\varepsilon_{p,s}$:

VON MISES or distortional energy criterion

$$\Delta\varepsilon_{eq}^{2} = 4\,\Delta\varepsilon_{p,n}^{2} + \frac{4}{3}\,\Delta\varepsilon_{p,s}^{2} \qquad (2)$$

TRESCA or maximum shearstrain criterion

$$\Delta\varepsilon_{eq}^{2} = \frac{16}{9}\,\Delta\varepsilon_{p,s}^{2} \qquad (3)$$

ST. VENANT or maximum principal strain criterion

$$\begin{aligned} \Delta\varepsilon_{eq} &= \Delta\varepsilon_{p,n} + \Delta\varepsilon_{p,s} \qquad -1 \leq \xi \leq 0 \\ \Delta\varepsilon_{eq} &= \Delta\varepsilon_{p,n} - \Delta\varepsilon_{p,s} \qquad 0 \leq \xi \leq 1 \end{aligned} \qquad (4)$$

The plastic strains at a certain number of cycles to failure have been determined by interpolation and plotted in a $(\Delta\varepsilon_{p,s},\Delta\varepsilon_{p,n})$-plane for WN 1.4948 at 550^0 (Figure 4). Comparison of the results with the criterions (2), (3) and (4) show that these criterions are conservative in the range $-1 \leq \xi \leq -0.5$. The same conclusion can be drawn for WN 1.4948 at 20^{0}C, WN 1.6770 at 550^{0}C. With the available testrig no experiments in the range $-0.5 \leq \xi \leq 1$ can be carried out. A literature survey for several materials /2,3/ showed that the recommended VON MISES criterion can be non-conservative in this region.

Based on the experimental results and on results from literature it is now proposed to use the criterion

$$\Delta\varepsilon_{eq}^{2} = (16-9\beta)\,\Delta\varepsilon_{p,n}^{2} + \beta\,\Delta\varepsilon_{p,s}^{2} \qquad (5)$$

where β is different for Case A and B and has to be determined experimentally. For $\beta = 4/3$ the criterion is equivalent to the VON MISES criterion and with $\beta = 16/9$ TRESCA criterion will be obtained. For $0 < \xi < 16/9$ the criterion is represented by an ellipse in the $(\Delta\varepsilon_{p,n}, \Delta\varepsilon_{p,s})$ plane which can give a good curve fit for Case A. In high-cycle fatigue GOUGH/4/ obtained a good description with an ellipse quadrant based on bending and torsion experiments, formulated in terms of stresses. For $\beta < 16/9$ a hyperbola is obtained which could be useful in approximating Case B. Note that for Case A $(\Delta\varepsilon_{p2} \geq \Delta\varepsilon_{p3})$ and Case B $(\Delta\varepsilon_{p2} \leq \Delta\varepsilon_{p3})$ the definitions of $\Delta\varepsilon_{p,n}$ and $\Delta\varepsilon_{p,s}$ are

Case A
$$\Delta\varepsilon_{p,n} = \frac{\Delta\varepsilon_{p1} + \Delta\varepsilon_{p2}}{2} \qquad \Delta\varepsilon_{p,s} = \frac{\Delta\varepsilon_{p1} - \Delta\varepsilon_{p2}}{2} \qquad (6)$$

Case B
$$\Delta\varepsilon_{p,n} = \frac{\Delta\varepsilon_{p1} + \Delta\varepsilon_{p3}}{2} \qquad \Delta\varepsilon_{p,s} = \frac{\Delta\varepsilon_{p1} - \Delta\varepsilon_{p3}}{2} \qquad (7)$$

For Case A we use the torsion test (ξ = -1) to determine β_A. With (5) one obtains

$$\beta_A = (\frac{2\Delta\varepsilon_{p,ax}}{\Delta\gamma_p})^2 \qquad (8)$$

where $\Delta\gamma_p$ is the plastic engineering shearstrain range at an equal number of cycles to failure as for the plastic strain range $\Delta\varepsilon_{p,ax}$ in a uniaxial test.

As no experimental results are available for the applied materials for Case B an extrapolation is made from Case A to Case B by assuming that the contour of equal fatigue life is smooth in the plane of principal surface strains ($\Delta\varepsilon_{p1}$ and $\Delta\varepsilon_{p2}$). Formulating (5) in terms of $\Delta\varepsilon_{p1}$ and $\Delta\varepsilon_{p2}$ for both cases and requiring that $d(\Delta\varepsilon_{p2})/d(\Delta\varepsilon_{p1})$ is the same for both cases at ξ = -0.5, yields

$$\beta_B = \frac{8}{3} - \beta_A \qquad (9)$$

Note that for β = 4/3 the VON MISES criterion is obtained for both Case A and B. The criterion (5) with parameter β defined by (8) and (9) has been applied for experimental data of a low-alloy ferritic steel given in literature /5/. Figure 5 shows that the criterion is conservative for all strain states, while criterions (2), (3) and (4) are nonconservative in the range $-0.5 \leq \xi \leq 1$. Figures 4 and 6 show the predictions with (5) in the ($\Delta\varepsilon_{p,s}$,$\Delta\varepsilon_{p,n}$)-plane and the ($\Delta\varepsilon_{p1}$,$\Delta\varepsilon_{p2}$)-plane respectivily for WN 1.4948 at 550°C. The experimental results for combined tension are well in agreement with the prediction. For WN 1.4948 at 20°C and WN 1.6770 at 550°C good agreement between experiment and prediction is obtained as well.

The equivalent strain (5) versus number of cycles to failure with parameter β_A which gave the best fit in a large range of number of cycles to failure is shown in Figure 7 for the applied materials. It is shown that with the proposed criterion multiaxial stress states in the range $-1 \leq \xi \leq -0.5$ can be related to uniaxial ones for this type of specimen. In the range $-0.5 \leq \xi \leq 1$ more experimental verification will be necessary.

4. Effect of specimen type on low-cycle fatigue life

Comparison of fatigue lives obtained in different laboratories is hampered by differences in testing technique, testing equipment, specimen geometry and surface finish. Diametrical strain control leads generally to higher lives than axial strain control, as for the latter higher local strains occur as a result of ridges and/or a curved gauge length. Comparison of the uniaxial test results obtained with tubular and solid specimens under identical test-conditions gives particularly for the ferritic steel considerable differences in fatigue life as is shown in Figure 8.

4.1 Effect of strain concentration

Elastic-plastic calculations have been carried out on both specimens with a TNO finite-element programma /6/ in which the description of material behaviour is based on the fraction or overlaymodel of BESSELING /7,8/. The calculations were verified by measurements at room temperature of the diametrical displacements at the smallest cross-section of a solid specimen (total axial strainrange 1.87 %). By elastic-plastic analysis an axial strain concentration factor (ratio of local strain to average strain over the gauge length) 1.72 was found, while by diametrical measurement a factor 1.75 was obtained. Measurement of longitudinal displacements of a 2 mm spacing grid on a tubular austenitic specimen again showed good agreement between experiment and calculation.

For both specimens of the ferritic steel a complete loadcycle at 550°C has been analysed. Results for average and local strains are shown in Figure 9. Figure 10 shows the calculated strain concentration on the surface of the solid specimen and for the outer and inner surface of the tubular specimen. As the highest strains occur on the inner surface it can be expected that the tubular specimens will fail by fracture initiated at the inner surface. The strain concentration on the inner surface of the tubular specimen is nearly equal to the strain concentration of the solid specimen. Therefore strain concentrations can not explain the difference in life time for both specimens.

4.2 Fracture characteristics

It is demonstrated in Figure 11a that the crack growth rate, determined by measurement of striation spacings of the fracture surface, shows large differences for both the steels and the types of specimen. Figure 11b shows another representation of the crack growth behaviour, obtained by dividing the crack length by a characteristic dimension (the radius of the cylindrical part for the solid specimen and the wall thickness for the tubular specimen). For both types of ferritic specimens the crack growth rate in relation to the normalized crack length is now nearly the same, from which it can be concluded that the difference in characteristic dimension is responsible for the difference in fatigue life.

For the austenitic steel the crack growth of the tubular specimen shows two stages (Figure 11b). The first stage shows a faint slope, the second stage shows a slope similar to the slope of the solid specimen. The difference in slope of the first and the second stage are well in agreement with the results of WAREING and VAUGHAN /9/. Due to a low surface roughness (tubular austenitic specimen about 1.5 Ru) relatively few cracks are initiated so that some constraint semi-circular cracks can grow. A change in crack growth behaviour will occur when neighbouring cracks interact. On the solid specimen (surface roughness 5-8 Ru) a continuous unconstrained front occurs all around the specimen circumference.
With unconstrained cracks a larger growth rate is found.

5. Conclusions

Results of biaxial low-cycle fatigue tests on thin-walled tubular specimens show that the classical criterions like VON MISES, TRESCA and ST.VENANT for relating a multiaxial stress state to a uniaxial one are conservative in the range of principal strainratios $-1 \leq \Delta\varepsilon_{p2}/\Delta\varepsilon_{p1} \leq -0.5$ for the two investigated materials.

With a parameter based on strains for equal fatigue life under push/pull loading and torsion a criterion has been derived which gives a good description for the experimental results and data from literature in the range of principal strainratios $-1 \leq \Delta\varepsilon_{p2}/\Delta\varepsilon_{p1} \leq -0.5$ Application of the criterion in the range $-0.5 \leq \Delta\varepsilon_{p2}/\Delta\varepsilon_{p1} \leq 1$, on result in literature for a low-alloy ferritic steel shows a better agreement than the classical criterions which are nonconservative for this ratios of principal strains.

Comparison of uniaxially loaded tubular and solid specimens showed a remarkable reduction in fatigue life for the tubular specimen, especially for the ferritic steel.

It is shown by experimentally verified elastic-plastic analysis that considerable strain-concentrations occur in both the tubular and the solid specimen. These concentrations are nearly the same for both specimens.

Differences in surface roughness can have a strong influence on crack initiation and crack growth. For the Nb-stabilized 2¼Cr1Mo steel differences in fatigue life were caused by the influence of specimen thickness on crack growth. For the 18Cr-11Ni steel this effect was compensated for the greater part by the lower surface roughness of the tubular specimen which caused less initiation sites and retardation of the first stage of crackgrowth with respect to the solid specimen.

6. Acknowledgements

This work was commissioned by the Project Group of Nuclear Energy TNO. The authors thank the Project Group and the Dutch Ministry of Economic Affairs for the permission to publish this paper.

References

/1/ ASME 1977 Code Cases, Nuclear Components, Case N-47, Class 1 components in elevated temperature service ASME, New York, (July 1977).

/2/ BROWN, M.W. and Miller, K.J. "A theory for fatigue failure under multiaxial stress-strain conditions", Proc. Inst. Mech. Eng., 187, 745-755 (1973).

/3/ KREMPL, E., "The influence of state of stress on low cycle fatigue of structural materials: a literature survey and interpretive report", Proc. ASTM, STP 549, 1974.

/4/ GOUGH H.J. and POLLARD, H.V. "The strength of materials under combined alternating stresses", Proc. Inst. Mech. Eng., 131, 3-, (1935).

/5/ PARSON, M.W. and PASCOE, K.J. "Low-cycle fatigue under biaxial stress", Proc. Inst. Mech. Eng., 188, 657-671, (1974).

/6/ OOSTERLING, C.R. and JANSSEN G.T.M., "CYPLAST, a finite-element computer programme for elastic-plastic analysis of axisymmetric and plane 2-dimensional structures", TNO-IWECO, Report no.: 5031025-78-2, (1978).

/7/ BESSELING, J.F. "A theory of elastic, plastic and creep deformation of an initially isotropic material showing anisotropic strain-hardening, creep, recovery and secondary creep", J. Appl. Mech., 25, 529 - 536, (1958).

/8/ MEIJERS, P., JANSSEN G.T.M. and BOOIJ J. "Numerical plasticity and creep analysis based on the fraction model and experimental verification for AISI 304", SMiRT III, paper L 3/9, London 1975.

/9/ WAREING, J. and VAUGHN H.G, "Influence of surface finish on low-cycle fatigue characteristics of type 316 stainless steel at 400°C", Metal Science, 13, 1-8, (1979).

Table 1 Chemical composition

material	product form.	chemical composition (wt. %)								
		C	Si	Mn	P	S	Cr	Ni	Mo	Nb
WN 1.4948	Ø 55 mm	0.044	0.68	1.94	0.022	0.006	18.1	10.9	0.37	n.d.
WN 1.6770	Ø 40 mm	0.050	0.2	0.62	0.010	0.007	2.0	0.66	0.85	0.82

Table 2 Mechanical properties

material	test temp. [°C]	tensile properties				Charpy. V impact [J]	hardness HV 10	grainsize acc.ASTM
		$R_{0.2}$ [MPa]	R_m [MPa]	A [%]	Z [%]			
WN 1.4948	RT	253	575	64	81	279	149	5-6
	550°C	130	310	30	74	-	-	-
WN 1.6770	RT	390	531	24	80	221	176	10
	550°C	271	327	13	83	-	-	-

Table 3 List of constants in COFFIN-MANSON relation $\Delta\varepsilon_{pl} = C.N_f^{\alpha}$

material	temp. [°C]	tension/compr.			tension/compr. + torsion			torsion		
		ξ	α	C	ξ	α	C	ξ	α	C
WN 1.4948	20	-0.5	-0.49	0.37	-0.83	-0.49	0.65	-1	-0.45	0.57
WN 1.4948	550	-0.5	-0.40	0.12	-0.78	-0.57	0.80	-1	-0.49	0.39
WN 1.6770	550	-0.5	-0.70	0.38	-0.81	-0.81	1.34	-1	-1.0	4.6

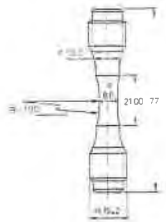

Figure 1 Solid test specimen

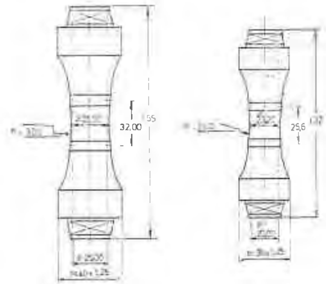

Tubular test specimen:

For the austenic For the ferritic steel

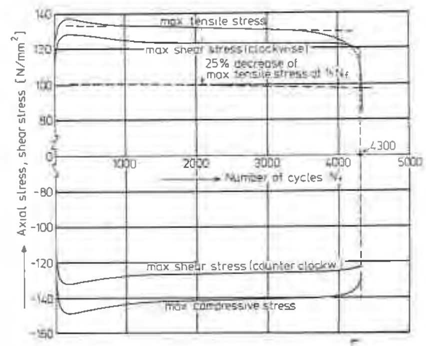

Figure 2 Stainhardening curves for WN 1.4948 tested at 550°C under biaxial conditions:

$\Delta\varepsilon_{ax} = 0.447$ %; $\Delta\gamma = 1.550$ %; $\Delta\varepsilon_{eq} = 1.0$ % (acc. VON MISES);

$\dot{\varepsilon}_{eq} = 1.5 \times 10^{-3} s^{-1}$

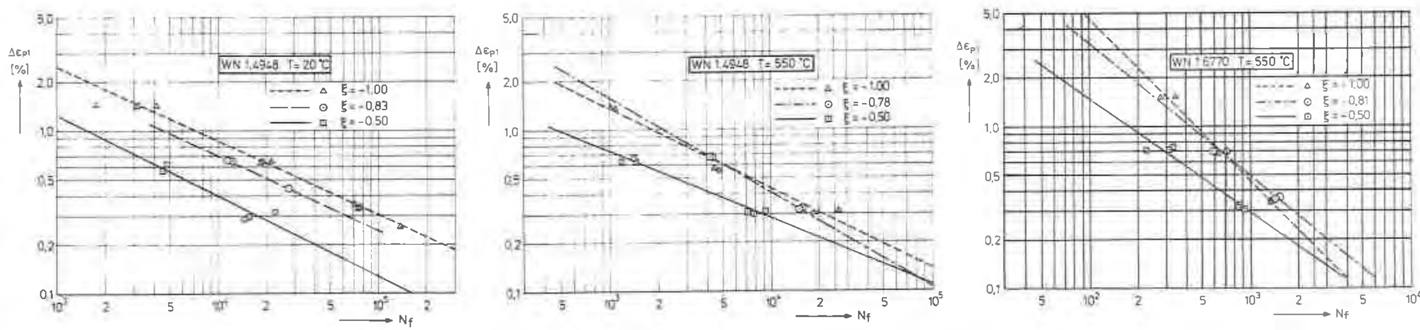

Figure 3 Number of cycles to failure versus largest plastic principal strainrage

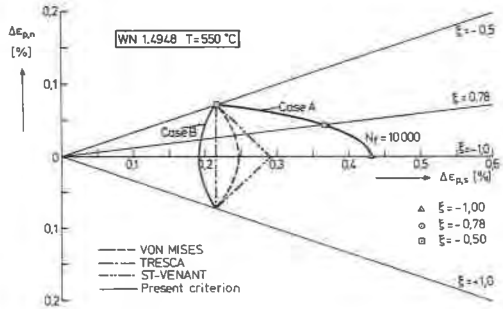

Figure 4 Comparison of failure models with experimental data

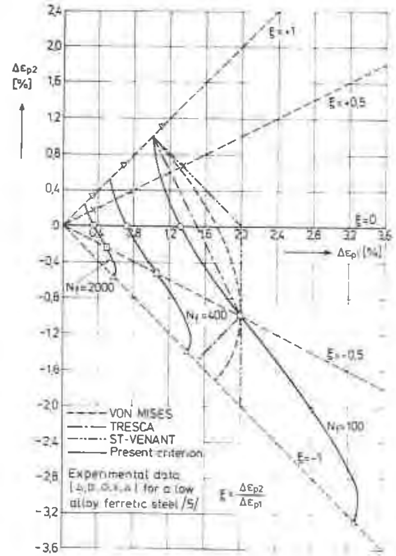

Figure 5 Experimental verification of failure models on plane of surface (plastic) strains

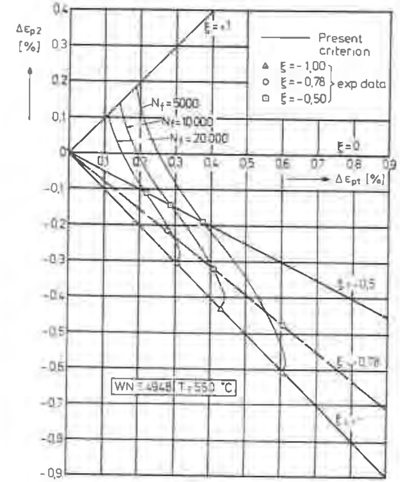

Figure 6 Contours of equal life compared with experimental data

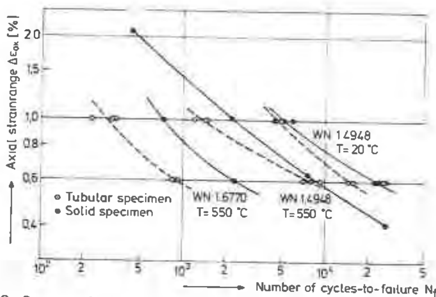

Figure 8 Comparison of fatigue life of Nb-stabilized $2\frac{1}{4}$Cr-1Mo (WN 1.6770) and 18Cr-11Ni steel (WN 1.4948), with tests on tubular and solid specimens

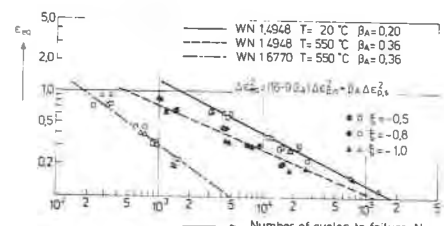

Figure 7 Equivalent strain versus number of cycles to failure.

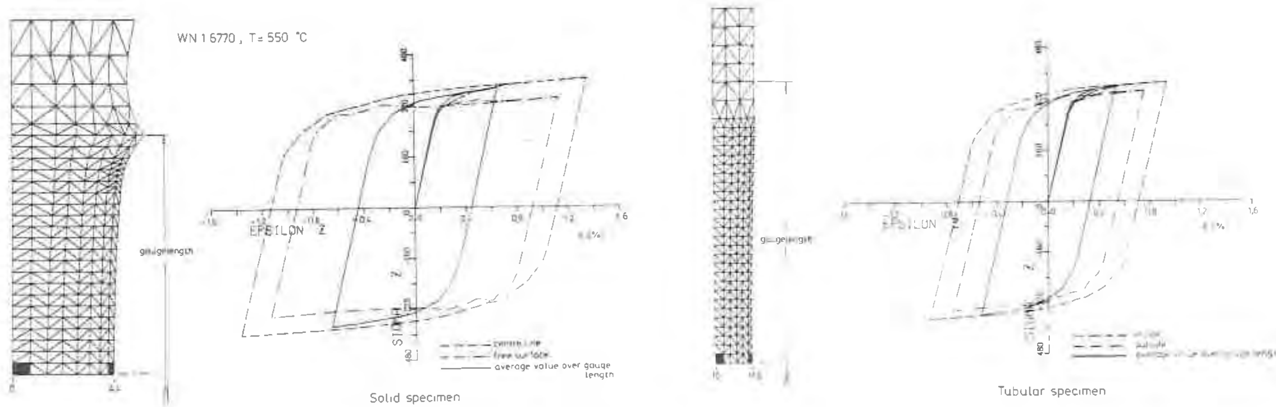

Figure 9 Calculated hysteresis loops

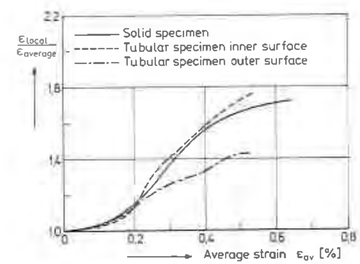

Figure 10 Strain concentration factor versus average strain, WN 1.6770, T=550°C.

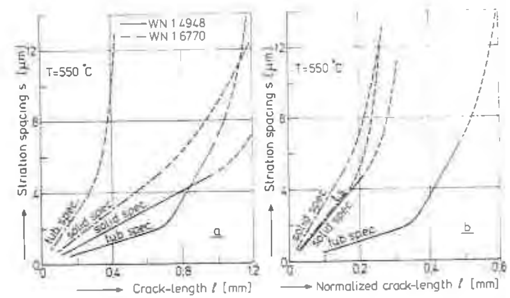

Figure 11 Striation spacing versus crack length.